HHS Public Access

Author manuscript

J Pathol. Author manuscript; available in PMC 2021 April 26.

Published in final edited form as:

J Pathol. 2019 October ; 249(2): 227–240. doi:10.1002/path.5311.

Loss of Rab25 promotes the development of skin squamous cell carcinoma through the dysregulation of integrin trafficking

Haengdueng Jeong[1,*], **Kyung-Min Lim**[2,*], **Kwang H. Kim**[1], **Yejin Cho**[1], **Buhyun Lee**[1], **Byron C. Knowles**[3], **Joseph T. Roland**[3], **Jeffrey P. Zwerner**[4], **James R. Goldenring**[3,5], **Ki Taek Nam**[1]

[1]Severance Biomedical Science Institute, Brain Korea 21 PLUS Project for Medical Science, Yonsei University College of Medicine, Seoul, 03722, Republic of Korea

[2]College of Pharmacy, Ewha Womans University, Seoul, 03760, Republic of Korea

[3]Epithelial Biology Center and Department of Surgery, Vanderbilt University School of Medicine and the Nashville VA Medical Center, Nashville, TN, 37232, USA

[4]Department of Dermatology, Vanderbilt University School of Medicine, Nashville, TN, 37232, USA

[5]Nashville VA Medical Center, Nashville, TN 37210, USA

Abstract

Rab25 functions as either a tumor suppressor or tumor promoter across different tissues. Here we have demonstrated and clarified the role of Rab25 as a pivotal tumor suppressor of the skin squamous cell carcinoma (SCC) development. Rab25 loss was closely associated with the neoplastic transition in both humans and mice. Rab25 loss was well correlated with increased cell proliferation and poor differentiation in human SCC. While Rab25 knock-out (KO) in mice did not induce tumor spontaneously, it significantly accelerated tumor generation and promoted malignant transformation in the mouse two-stage skin carcinogenesis model *in vivo*. Xenograft of a Rab25 deficient-human keratinocyte cell line, HaCaT, also elicited the neoplastic transformation. Notably, Rab25 deficiency led to dysregulation of integrin β1, β4 and α6, which matched well with increased epidermal proliferation and apoptosis, and impaired desmosome-tight junction formation. Rab25 deficiency induced impairment of integrin recycling, leading to the improper expression of integrins. In line with this, significantly attenuated expression of integrin β1, β4 and α6 was identified in human SCC where Rab25 was deficient. Collectively, these results suggest that loss of Rab25 promotes the development and neoplastic transition of SCC through dysregulation and trafficking of integrins.

Address correspondence to: Ki Taek Nam, D.V.M., Ph.D., Severance Biomedical Science Institute, Yonsei University College of Medicine, 50-1 Yonsei-ro, Seodaemun-gu, Seoul, 03722, Republic of Korea, kitaek@yuhs.ac; or James R. Goldenring, M.D., Ph.D., Epithelial Biology Center and Department of Surgery, Vanderbilt University School of Medicine, 10435-G MRB IV, 2213 Garland Ave, Nashville, TN 37232. jim.goldenring@vanderbilt.edu.

*These authors contributed equally to this work.

Statement of author contributions

HDJ, KML, JRG, and KTN designed research studies, HDJ, KHK, YJC, and BHL conducted experiments, HDJ acquired data, HDJ, KML & KTN analyzed data, BCK, JTR, JPZ and JRG provided reagents, and HDJ, KML, KTN, & JRG wrote the manuscript.

Conflict of Interest statement: The authors state no conflict of interest

Keywords

Rab25; skin; epidermis; squamous cell carcinoma (SCC); integrin

Introduction

Rab25, a member of the Rab11 small GTPase family, regulates trafficking of integral membrane proteins (EGFR, α6β1 integrin) and receptors, which are critical to the maintenance of polarity in epithelial cells [1,2]. As Rab25 is highly expressed in epithelial cells, Rab25 deficiency in epithelial cancer elicits aggressive behaviors including human colon cancer [3,4], triple negative breast cancer cell and human mammary cancer tissues [5,6], and HNSCC [7], supporting that Rab25 may work as a crucial tumor suppressor in epithelial cancers.

Interestingly, in some human cancers including liver cancer [8], breast cancer, and ovarian cancer [9], dysregulated overexpression of Rab25 proteins is observed [10]. Oncogenic outcome elicited by Rab25 overexpression may be mediated through the activation of AKT signaling, resistance against metabolic stress [11], and recycling of receptor tyrosine kinases and α5β1 integrins [12], engendering cancers more prone to metastasis and invasion. These hypotheses contrast with observations in colon and breast cancer, where tumor suppressor effects are noted [3,4,13], reflecting that role of Rab25 in carcinogenesis may diverge across tissues.

The skin epidermis is composed of 4 layers of squamous epithelial cells, which are derived from the stem cell rich region located at basal layer. The basal layer maintains the epidermal homeostasis and is enriched with quiescent stem cells and transit-amplifying cells, orchestrating the regeneration of skin epidermis [14,15]. Each layer of the skin epidermis expresses distinctive markers, such as desmosomes, filaggrin, loricrin, involucrin, keratin family and integrins, which are critical for well-orchestrated differentiation and functional maturation of the skin barrier into corneocytes. Integrins α6, β4, and β1 are expressed in the basal cell layer and hair follicles where keratinocyte proliferation from epidermal stem cells is highly active, reflecting their essential roles in keratinocyte differentiation and proliferation. Deletion of these integrins *in vivo* leads to diverse skin disorders [16–18]. Especially, in squamous cell carcinoma (SCC), loss of integrins is well established [19], and focal integrin loss is closely associated with poor differentiation, malignant transformation and invasiveness of SCC [20,21]. Despite the abundance of evidence supporting the critical role of integrin regulation in SCC, the mechanisms underlying it remain largely unidentified.

Here we have determined that Rab25 functions as a tumor suppressor for skin squamous cell carcinoma development. We confirmed the significant negative correlation of Rab25 expression with human skin SCC. The tumor suppressive effects of Rab25 in the skin tumorigenesis were demonstrated in Rab25 KO mice, which showed acceleration of the squamous cell-derived tumor generation in the two-stage carcinogenesis model. Of note, integrins were significantly dysregulated, which coincided with Rab25 deficiency. We studied the mechanism underlying the tumor-suppressive effects of Rab25 on skin SCC

development to provide important insights into understanding the role of Rab25 in the development of skin cancers.

Materials and Method

Mice

All animal experiments were conducted in accordance with the Public Health Service Policy in Humane Care and Use of Laboratory Animals and were approved by the IACUC of the Department of Laboratory Animal Resources of Yonsei University College of Medicine, an AAALAC-accredited unit (#001071). 5 to 9-week-old 129/J background mice, maintained in specific pathogen-free conditions (SPF), were used for all experiments. Rab25 KO mice were genotyped as previously described. [3].

Skin tumorigenesis experiments

For DMBA/TPA-induced skin carcinogenesis, mice were carefully shaved and a single dose of DMBA (0.1 μmol in 200 μl acetone, Sigma) was topically applied to mouse back skin. Application of TPA (20 nmol in 200 μl acetone, Sigma) was initiated 1 week after application of DMBA. Groups of mice were treated with twice-weekly applications of TPA for the duration of the experiment. All carcinogenic chemical was gently rubbed for soaking the whole dorsal skin of mouse. Tumor size and the number of papilloma were measured every week under anesthesia. A total of 49 mice were divided into four groups (DMBA/TPA treated, DMBA only treated, TPA only treated, Vehicle treated). (Figure S1A)

Establishment Rab25 Knockdown cell lines

Recombinant lentiviruses were commercially designed and synthesized using GIPZ lentiviral shRNA vector (Open Biosystems, Huntsville, USA). Lentiviruses were produced by transfection of 293T cells with packaging plasmids PMD2G and psPAX2, using a Calphos™ Mammalian Transfection Kit (Clontech, 631312) according to the manufacturer's protocol. Knockdown of Rab25 in HaCaT cell was established by infection of recombinant lentivirus using a polybrene mixture. Stable clones expressing shRNA were selected via further incubation with puromycin (1 μg/ml) and fluorescence expression of GFP.

Immunocytochemistry

For immunocytochemistry, cells were seeded on Poly-L-lysine (Sigma, P7407) coated 24 well Chamber slides, grown until 80~90% confluency and fixed with 4% PFA for 15 min. Fixed monolayer cells were washed twice with ice-cold PBS and incubated with 0.25% Triton X-100 in PBS for 15 min for permeabilization. Cells were incubated with 1% BSA for 30 min for blocking of non-specific binding, followed by primary antibodies at 4°C overnight. After 2 washes in ice-cold PBS, primary antibodies were detected with cy3-conjugated anti-mouse IgG and cy5-conjugated anti-rabbit IgG (Jackson Laboratories), followed by DAPI staining. Confocal images were taken with a Zeiss LSM 800 and LSM780 confocal microscope using Zeiss software (Carl Zeiss Micro Imaging, Jena, Germany). The assessment of integrin internalization was performed as described in supplementary material and method.

Immunoblot

For immunoblot for cell line, cells were harvested and incubated in protein lysis buffer (20 mM Tris (pH 7.4), 0.15 M NaCl, 2.5 mM EDTA, 1% Triton X-100) for 40 min. For immunoblot for mice skin, mice were shaved and euthanized in a CO_2 chamber. The skin was carefully cut and collected in 1.5 ml microtubes. Proteins were extracted from sections with protein lysis buffer (20 mM HEPES (pH 7.0), 0.15 M NaCl, 10% Glycerol, 1% Triton X-100, 1 mM EDTA, 1 mM EGTA, 10 mM β-phosphoglycerate) with protease and phosphatase inhibitor cocktails (Thermo, MA, USA). All lysates were collected by centrifugation (13000 rpm, 15 min) and boiled in 1X SDS-PAGE sample buffer (62.5 mM Tris–HCl (pH 6.8)), 2 % SDS, 5 % β-mercaptoethanol, 10 % glycerol, 0.01 % bromophenol blue) after measurement of protein concentration. 20 μg protein samples were separated by SDS-PAGE and transferred to a PVDF membrane (Millipore, Billerica, USA). The membranes were incubated overnight at 4°C with primary antibodies. Signal intensities were measured using image analysis software, Image J (developed by Wayne Rasband).

Clinical data analysis using human skin tissue microarray

For skin tissue microarray (TMA), immunohistochemistry was performed as described in supplementary material and method. The images were taken using an Aperio Versa imager (Vanderbilt Digital Histology Shared Resource). The evaluation of the staining was conducted using Tissue image analysis 2.0 (Leica). Intensity for DAB positive area of Rab25 and integrins analyzed by immunohistochemistry staining. The detailed method of immunohistochemistry was performed as described in supplementary material and method.

Statistical analysis

Data are presented as mean ± SEM. Statistical significance was determined using unpaired Student's t test or one-way ANOVA with Dunnett's multiple comparison. Kaplan-Meier survival analysis was used to compare squamous cell carcinoma patient survival by the log-rank test. $P<0.05$ was considered significant. $*P<0.05$; $**P<0.01$; $***P<0.001$

Results

Rab25 expression in human skin squamous cell carcinoma

A tissue microarray (TMA) of human skin precancerous and cancerous lesions was examined for Rab25 expression. As shown in Figure 1A, the intensity of Rab25 staining was reduced in the full gamut of skin SCC-related lesions, including precancerous actinic keratosis, human papillomavirus-associated SCC *in situ* (SCCIS), bowenoid papulosis and invasive SCC. Notably, the intensity of Rab25 staining was significantly lower in invasive SCC arising within SCCIS (iSCC/SCCIS) than other precancerous lesions (Figure 1A). Immunofluorescence staining clearly showed localization of Rab25 in epidermis. In normal human skin, Rab25 expression was found in cells within the basal and granular layers of the epidermis, where intracellular vesicle trafficking and secretion are highly active (Figure 1B). Although the skin SCC, regardless of differentiation level, revealed reduced Rab25 expression compared with normal skin, Rab25 expression was preserved in some skin SCC

with relatively well-differentiated borders, further substantiating that Rab25 which expressed in the skin epidermis negatively correlated with development of SCC (Figure 1C).

Loss of Rab25 promotes skin-tumor development in the two-stage tumorigenesis mouse model

To elucidate further the role of Rab25 in the development of skin squamous cell carcinoma, we employed the DMBA/TPA-induced two stage skin carcinogenesis mouse model (Figure S1A) using wild type (WT) and Rab25 KO mice. As shown in Figure 2A and 2B, macroscopic observation revealed that at 10 weeks post-DMBA treatment, while no skin tumors were generated in WT mice (left panel), Rab25 KO mice developed tumors (right panel) (Figure 2A). At 20 weeks, Rab25 KO mice (right panel) showed skin tumors with larger sizes and in larger numbers compared with WT mice (left panel) (Figure 2B). Indeed, Rab25 KO significantly and potently stimulated the development of skin tumors with respect to the size and the number at the terminal observation and the latency of first tumorigenesis (Figure 2C and 2D).

Loss of Rab25 promotes squamous cell carcinoma in mouse tumorigenesis model

Skin from all of the mice underwent histopathological examination based on the WHO IARC classification criteria [22]. The malignancy was scored by categorizing skin lesions or skin tumor into squamous cell hyperplasia, squamous cell papilloma and squamous cell carcinoma as diagnosed by pathologists (Figure S2A–S2D). Detailed criteria are described in the Supplementary materials and methods. Most of SCCs were well-differentiated tumors showing ample keratin production, and the keratin formed characteristic structures termed keratin pearls (KP) that were composed of concentric layers of squamous cells around central layers of keratin. (Figure S2D, KP) The basal layers have frequent mitotic figures that were often irregular, formed buds and nests, or consisted of few cells. (Figure S2D, insert box)

Collectively, in the mouse two-stage skin carcinogenesis model, it was revealed that most of Rab25 KO mice developed more severe forms of skin tumors, namely papilloma and SCC than WT (Figure S2 and Table 1 and 2). All the Rab25 KO mice developed papilloma and 9/15 showed SCC, while SCC was observed in only one WT mice (1/10). Interestingly, TPA-treatment without DMBA induced papilloma development in Rab25 KO mice, while only hyperplasia was observed in WT (Table 1).

Rab25 expression gradually disappears during skin tumorigenesis

We examined the alteration in the distribution of Rab25 expression in the epidermis during the course of tumor development. As shown in Figure 2E, in the untreated normal mice skin, Rab25 was diffusely and strongly expressed throughout epidermis while no staining was observed in the dermis. In contrast, in the region adjacent the tumor where epidermal hyperplasia was observed, Rab25 expression was attenuated and detected sparsely around corneal and basal cell layer (Figure 2F). Strikingly, in the tumor regions, Rab25 was hardly detectable (Figure 2G), strongly reflecting the pivotal association of Rab25 loss with skin tumorigenesis. As expected, Ra25 was not detected in untreated and DMBA/TPA treated epidermis of Rab25 KO mice. (Figure S1B)

Increased proliferation and apoptosis in the skin epidermis of untreated Rab25 KO mouse

As described above, the skin squamous cell tumor lesions in the two-stage carcinogenesis model showed significantly more severe and hyperplasic features of skin tumor development in Rab25 KO mice. To assess further cell proliferation and apoptosis in the Rab25 KO mouse, we conducted BrdU and TUNEL staining in the untreated skin. As shown in Figure 3A and 3B, the number of proliferating cells were prominent in Rab25 KO mice. Along with increased cell proliferation, apoptosis was also promoted in Rab25 KO mice (Figure 3C and 3D). Both $BrdU^+$ and $TUNEL^+$ cells increased by ~ 3-fold in Rab25 KO compared to WT (Figure 3B and 3D).

To investigate the morphological alteration of proliferating cells, which are enriched in the basal layer, transmission electron microscopic (TEM) examination was conducted. TEM image of the skin showed spreading cell shapes in the basal layer of Rab25 KO and fewer desmosome complexes in the epidermis of Rab25 KO compared with WT mice. (Figure S3A and S3B). qPCR data revealed that the expression of components of desmosome complex (DSG2, DSC1) was down-regulated in untreated Rab25 KO mice, but DSG1 was not affected (Figure S3C). Collectively, Rab25 deficiency led to increased cell proliferation as well as apoptosis in the basal layer of skin epidermis, which would promote the skin turnover significantly.

Identifying integrin distribution in the basal layer of WT and Rab25 KO mice

During epithelial cell carcinogenesis, loss of integrin frequently occurs. In addition, integrins are the major target molecules governed by Rab25 regulation. We examined the expression of α6, β4, and β1 integrin, all of which are critical in the regulation of skin regeneration and skin malignancy [21]. As shown in Figure 4A, those integrins were enriched in the basal layer of the epidermis of WT mice, where β4 and β1 appeared as dispersed throughout the basal cells, while α6 showed a sparse and focal staining pattern in the perinuclear and nuclear region of specific groups of basal cells. The integrin expression could be confirmed in the epidermis of WT mice, but the expression of all three integrins exhibited substantially attenuated and less focused features in Rab25 KO mouse epidermis (Figure 4A). Immunoblot assay further corroborated the reduced integrin expression in the skin of Rab25 KO mice (Figure 4B and 4C). In contrast, in the skin dermis, α6 integrin was strongly expressed, while β1 and β4 integrin had weak or no staining intensity (Figure 4A). Interestingly, Rab25 deficiency did not affect integrin expression in skin dermis. Since both Rab25 and integrins were enriched in basal cells of epidermis through immunohistochemistry, we examined whether Rab25 and integrins existed in the same cellular loci. Immunofluorescence staining showed that Rab25, which is highly expressed in whole basal cell layer, was co-localized with β4 and β1 integrin in those cells (Figure 4D), while not with α6 integrin.

Furthermore, we conducted immunofluorescence staining for BrdU (proliferating cell marker) and α6 integrin located in the stem cell region. Interestingly, proliferating cells were not co-localized with α6 integrin positive cells and the number of α6 integrin positive cells and BrdU positive cells were inversely correlated in WT and Rab25 KO (Figure S4A and

S4B). This result indicates that dysregulated α6 integrin expression may be linked with increased cell proliferation in Rab25 KO mice.

Downregulation of Rab25 in HaCaT cells promoted proliferation and integrin deficiency

To confirm the tumor-suppressive effects of Rab25 in skin tumors, we examined the effects of Rab25 deficiency on the tumorigenicity of HaCaT cells, a human keratinocyte cell line. Infection of HaCaT cells with lentiviral vectors conveying Rab25 knock-down (KD1 and KD2) sequence led to increased cell proliferation (Figure S5A). Consistently, HaCaT cells infected with Rab25 KD1 and KD2 showed complete suppression of Rab25 expression as well as significant downregulation of β1, β4, and α6 integrins (Figure S5B and S5C).

To examine if Rab25 KD may influence tumorigenicity of HaCaT cells, xenografting was conducted in nude mice. Inoculation of a large number of HaCaT cells can generate tumor-like lesions [23,24]. We also could observe the xenograft tumor tissues originating from HaCaT cell in nude mice. Rab25 KD in HaCaT cells led to significant increases in the size of tumors generated when compared with wild type (WT) or vector control (Con) cell lines. (Figure S5D). Interestingly, Rab25 KD cell-derived tumors also showed down-regulated expression of β1, β4, and α6 integrins (Figure S5E). Furthermore, the lesions of WT and vector control cell line-derived tumors showed well-differentiated morphology spanning from basal to cornified layers, expressing high levels of keratin14, keratin10 and loricrin (Figure S6). But Rab25 KD cell-derived lesions exhibited poorly differentiated morphology and lower expression of skin differentiation markers, which is characteristic of more malignant skin tumors (Figure S6), confirming that Rab25 deficiency promotes tumorigenicity in an integrin-dependent fashion regardless of experimental models.

Rab25 associates with β1 and β4 integrins in the perinuclear region of HaCaT cells

To understand the regulation of integrins by Rab25, we examined the distribution of the three integrins and Rab25 by immunocytochemistry using HaCaT cells. Rab25 localized only in the cytoplasm of HaCaT cells (Figure 4E–G). β1 integrin was expressed in both nuclear and cytoplasmic regions, where the stronger staining was observed in nuclear and perinuclear regions of WT and control lentiviral-infected HaCaT cells. β1 integrin co-localized with Rab25 in perinuclear region (Figure 4E). On the other hand, β1 integrin expression almost disappeared in Rab25-depleted human keratinocytes (Figure 4E, right panel: Rab25 KD). Meanwhile, β4 integrin appeared diffusely in cytoplasm and in a concentrated fashion in perinuclear region, where it was co-localized with Rab25 (Figure 4F). Rab25 KD led to substantial reduction of β4 integrin expression especially in the perinuclear region (Figure 4F, right panel). α6 integrin appeared both in cytoplasm and nucleus, but showed weaker perinuclear staining as compared with β1 or β4. Rab25 KD resulted in a significant reduction of α6 integrin, especially in the cytoplasm. However, co-localization with Rab25, as shown for β1 and β4, was not observed for α6 integrin (Figure 4G).

Altered integrin distribution in Rab25 knock-down HaCaT cells

Based on our previous data, we postulated that alteration of Rab25-dependent recycling pathways was associated with the loss of integrin. To clarify this speculation, we examined

the distribution of integrins in endosomal compartments (early endosome, late endosome, recycling endosome). Captured confocal images were analyzed using the co-localization evaluation module of the built-in Zeiss software, where co-localizing pixels above threshold are represented by white dots. Three representative markers were used for this experiment: Rab5a (early endosome marker), Rab7a (late endosome marker and a pre-requisite for phago-lysosome pathway) and Rab11a (recycling endosome marker). As shown in Figure 5A, the proportion of β1 integrin in Rab11a-containing recycling endosomes (right panel) was significantly decreased in Rab25 KD compared with WT, while the proportion of β1 integrin in late endosomes (middle panel) increased conversely. The proportion of β4 integrin in endosomes showed a similar pattern as observed for β1 integrin (Figure 5B). However, the proportion of β1 integrin and β4 integrin in Rab5a-positive early endosomes (left panel) was not affected by Rab25 KD (Figure 5A and 5B). Even with Rab25 expression decreased, expression of Rab11a and Rab11b, Rab11 protein family members with Rab25, did not diminish in either mouse skin or HaCaT cells (Figure S7A and S7B), indicating that decreased integrin expression was not caused by alteration of Rab11a or Rab11b expression. Interestingly, there was no difference between WT and Rab25 KD in internalization of α6 integrin, which did not co-localize with Rab25 (Figure 5C). These results suggest that Rab25 selectively regulated the recycling pathways of β1 and β4 integrin without affecting Rab11a or Rab11b expression and loss of Rab25 facilitated trafficking into late endosomes rather than activating recycling.

Integrins are markedly reduced in cancer region of human skin cancer.

Integrin expression appeared to be key to Rab25-mediated tumor suppressive effects. To further investigate the integrin expression in SCC, the human skin cancer TMA, as probed Rab25 (Figure 1A), was examined for integrin expression and distribution. In normal human tissues, all three integrins were expressed in basal layer cells and especially α6 integrin was strongly stained in a subset of basal cells, as was the cases in mouse tissue (Figure 6A and 6B). In contrast, in SCC lesions where Rab25 was downregulated, β1 and β4 integrin nearly disappeared in the basal cell layer. α6 integrin in SCC *in situ* was attenuated, and redistributed from perinuclear region into the cell membrane. This pattern could be also observed in mouse in a similar fashion (Figure 6A and 6B). Quantitation of staining intensity for integrins confirmed that β1 and β4 integrins were significantly lower in SCC than normal human skin (Figure 6C). Interestingly, expression of α6 integrin was significantly lower in the early cancer legion, SCC *in situ*, but this difference was dissipated in SCC (Figure 6C). There was a hint of an altered cellular localization in some SCC and certain regions of epidermis, which is in line with the re-localization of integrin in the terminal phase of epithelial cell carcinogenesis [25]. Taken together, our results demonstrated that Rab25 was highly and extensively expressed in human and mouse keratinocytes especially in basal cells, helping to maintain keratinocyte integrity and differentiation, which may be mediated by regulating proper integrin recycling. Deficiency of Rab25 induces an alteration of integrin distribution, ultimately increasing the tumorigenicity. (Figure 6D)

Discussion

Contradictory reports continue with regard to the role of Rab25 in tumorigenesis. Our group showed that loss of Rab25 in the intestine reduced basolateral presentation of β1 integrin in intestinal enterocytes [3], suggesting that alteration of Rab25 may disrupt the polarization of epithelial cells as well as induce directional alteration in integrin expression. These findings were confirmed in Caco-2 cells with knockdown of Rab25 expression [13]. In contrast, Rab25 is known to function as an oncogene in ovarian and luminal breast cancers [26,27]. Furthermore, Jeong et al. found that the oncogenic activity of Rab25 in ovarian cancer cell lines accrued through Rab25-dependent increases in β1 integrin levels, which subsequently activate EGFR, upregulate VEGF-A expression and increase Snail expression, ultimately promoting cancer cell invasion [28]. Those data suggest that while Rab25 regulates trafficking in many cells, the actual patterns of integrin regulation are dependent on tumor context. In tumors originated from HNSCC [7,29], oral SCC [30], oropharyngeal SCC and esophageal SCC [31], tumor suppressor effects of Rab25 are well-established. This conclusion is supported by clinical outcome of high Rab25 expression with positive prognosis in the patients with HNSCC [32]. However, the role of Rab25 in the squamous epithelia of skin was previously unknown.

Here we have demonstrated and clarified the novel role of Rab25 as a significant tumor suppressor in the skin SCC, where Rab25 loss is closely associated with the promotion of tumor generation from the early phase of squamous cell hyperplasia. This pattern was confirmed in Rab25 KO mice and human skin SCC, where Rab25 loss is well correlated with increased cell proliferation and poor differentiation. Furthermore, we also identified the enrichment of Rab25 expression in the basal layer of the epidermis, where epidermal stem cells reside with a gamut of integrins governing cell proliferation and cell-ECM interactions. However, as with previous reports, Rab25 knock-out alone did not induce spontaneous tumorigenesis [3,25].

Integrins exist in epidermal basal cells, interacting with basement ECM components like laminin and collagens [33,34]. The basal cells of the skin epidermis are pivotal to the regulation of keratinocyte proliferation and terminal differentiation, which is integral to the maintenance of skin integrity [14,35]. Sequential loss of integrin β1, α6 and subsequent disengagement from cell-ECM interaction in basal cells is the signature of terminal differentiation [36,37]. Consequently, the dysregulation of the integrin turnover can lead to diverse skin disorders as evidenced in integrin KO mouse studies [16–18]. Indeed, we found global decreases in integrin expression in human SCC which are attributable at least in part to loss of Rab25. Loss of Rab25 in mice and HaCaT cells induced overall decreases of β1, α6 and β4 integrins, consistent with increased cell proliferation and the promotion of tumor progression in the skin. Interestingly, TEM images showed abnormal morphology of basal cells in the Rab25 KO mice and the loss of desmosome complex. While, those finding may be related to skin integrity and neoplastic transition, further investigation is needed regarding correlation with loss of Rab25 and aberrant basal cell morphology including desmosome deficiency.

We postulated that loss of Rab25 may impair the proper regulation of cell proliferation and differentiation through the dysregulation of integrin, as Rab25 exists in recycling endosomes along with other Rab11 family proteins [2], which process a number of membrane cargoes including integrins and EGFR [12,38]. We provided a high-resolution image of keratinocytes with confocal microscopy, which revealed the co-localization of integrins with Rab25 in the basal layer of the skin epidermis. Rab25 exists in abundance around perinuclear region where recycling endosomes are active. In the perinuclear region, Rab25 was co-localized with β1 and β4 integrins, reflecting that Rab25 may be involved in the recycling of these integrins. Depletion or deficiency of Rab25 resulted in impaired integrin distribution, which we demonstrated with Rab25 KO mice and Rab25 KD HaCaT cells. As elaborated above, impairment of integrin recycling would lead dysregulated integrin turnover, which would impair proper integrin presentation at the cell membrane, and ultimately disrupt epithelial polarization, making conditions favorable for tumor malignancy and invasion.

Interestingly, while α6 integrin was also down-regulated in Rab25 KO mice and Rab25 KD HaCaT cells, localization with Rab25 as shown with β1 and β4 integrins, was not observed, indicating that α6 integrin may be indirectly regulated by Rab25. Indeed, ablation of β1 also causes the down-regulation of α6 and β4 integrins [37].

In addition, α6 integrins present in the nucleus, where Rab25 does not exist, would have a function distinct from that in the cytoplasm or perinuclear regions. Lathia et al. reported that α6 integrin, forming heterodimers with integrin β1 or β4, marks glioblastoma stem cells which work as a receptor for the ECM protein laminin [39]. Of note, α6 positive cells mark quiescent stem cells in the human skin epidermis [14]. and recent study also revealed that the existence of a heterogeneous stem cell population in the mouse epidermis and some long-lived stem cell populations were shown to highly express integrins [40]. We have provided evidence suggesting that α6 integrin may mark quiescent stem cell in the mouse skin epidermis by double staining with BrdU incorporation. Although intracellular alteration of α6 integrin may be closely linked with stem cell composition and tumorigenesis, further investigation needs to be supported using other stem cell markers such as Lrig1.

Collectively, our study provides an important line of evidence supporting the tumor suppressor effects of Rab25 in the skin SCC, where the loss of Rab25 promoted the cell proliferation and tumor generation. Dysregulated integrins may be closely involved in the mediation of enhanced tumorigenesis associated with loss of Rab25 expression, which corroborates the previous findings in colon cancer. Further study is warranted for the elucidation of the mechanisms regulating integrin trafficking by Rab25 and its association with epithelial tumor development in various settings.

Supplementary Material

Refer to Web version on PubMed Central for supplementary material.

Acknowledgements

This research was supported by the Korea Mouse Phenotyping Project (NRF-2016M3A9D5A01952416) of a National Research Foundation grant funded by the Korean government (MSIP), the Brain Korea 21 PLUS Project

for Medical Science at Yonsei University (to K.T.N.) JRG was supported by grants from the NIH (RO1 DK48370 and R21 CA187307). Production of the skin cancer TMA was supported in part by the Vanderbilt CTSA grant UL1 TR000445 from NCATS/NIH and was constructed in the Translational Pathology Shared Resource using a Grandmaster robotic arrayer acquired through NIH S10 OD016355. This work was supported by core resources of the Vanderbilt Digestive Disease Center, (P30 DK058404) the Vanderbilt-Ingram Cancer Center (P30 CA68485), and imaging in the Vanderbilt Digital Histology Shared supported by a VA Shared Instrumentation grant (1IS1BX003097). The authors would like to thank Dong-su Jang, MFA, (Medical Illustrator) for his help with the illustration.

Reference

1. Wang X, Kumar R, Navarre J, et al. Regulation of vesicle trafficking in madin-darby canine kidney cells by Rab11a and Rab25. J Biol Chem 2000; 275: 29138–29146. [PubMed: 10869360]
2. Welz T, Wellbourne-Wood J, Kerkhoff E. Orchestration of cell surface proteins by Rab11. Trends Cell Biol 2014; 24: 407–415. [PubMed: 24675420]
3. Nam KT, Lee HJ, Smith JJ, et al. Loss of Rab25 promotes the development of intestinal neoplasia in mice and is associated with human colorectal adenocarcinomas. J Clin Invest 2010; 120: 840–849. [PubMed: 20197623]
4. Goldenring JR, Nam KT. Rab25 as a tumour suppressor in colon carcinogenesis. Br J Cancer 2011; 104: 33–36. [PubMed: 21063400]
5. Cheng JM, Ding M, Aribi A, et al. Loss of RAB25 expression in breast cancer. Int J Cancer 2006; 118: 2957–2964. [PubMed: 16395697]
6. Cheng JM, Volk L, Janaki DK, et al. Tumor suppressor function of Rab25 in triple-negative breast cancer. Int J Cancer 2010; 126: 2799–2812. [PubMed: 19795443]
7. Seven D, Dogan S, Kilic E, et al. Downregulation of Rab25 activates Akt1 in head and neck squamous cell carcinoma. Oncol Lett 2015; 10: 1927–1931. [PubMed: 26622777]
8. He H, Dai F, Yu L, et al. Identification and characterization of nine novel human small GTPases showing variable expressions in liver cancer tissues. Gene Expr 2002; 10: 231–242. [PubMed: 12450215]
9. Cheng KW, Lahad JP, Gray JW, et al. Emerging role of RAB GTPases in cancer and human disease. Cancer Res 2005; 65: 2516–2519. [PubMed: 15805241]
10. Mitra S, Cheng KW, Mills GB. Rab25 in cancer: a brief update. Biochem Soc Trans 2012; 40: 1404–1408. [PubMed: 23176489]
11. Cheng KW, Agarwal R, Mitra S, et al. Rab25 increases cellular ATP and glycogen stores protecting cancer cells from bioenergetic stress. EMBO Mol Med 2012; 4: 125–141. [PubMed: 22253197]
12. Dozynkiewicz MA, Jamieson NB, Macpherson I, et al. Rab25 and CLIC3 collaborate to promote integrin recycling from late endosomes/lysosomes and drive cancer progression. Dev Cell 2012; 22: 131–145. [PubMed: 22197222]
13. Krishnan M, Lapierre LA, Knowles BC, et al. Rab25 regulates intergrin expression and trafficking in polarized colonic epithelial cells. Molec. Biol. Cell 2013; 24: 818–831. [PubMed: 23345591]
14. Solanas G, Benitah SA. Regenerating the skin: a task for the heterogeneous stem cell pool and surrounding niche. Nat Rev Mol Cell Biol 2013; 14: 737–748. [PubMed: 24064540]
15. Hsu YC, Li L, Fuchs E. Transit-amplifying cells orchestrate stem cell activity and tissue regeneration. Cell 2014; 157: 935–949. [PubMed: 24813615]
16. Dowling J, Yu QC, Fuchs E. Beta4 integrin is required for hemidesmosome formation, cell adhesion and cell survival. J Cell Biol 1996; 134: 559–572. [PubMed: 8707838]
17. Georges-Labouesse E, Messaddeq N, Yehia G, et al. Absence of integrin alpha 6 leads to epidermolysis bullosa and neonatal death in mice. Nat Genet 1996; 13: 370–373. [PubMed: 8673141]
18. Brakebusch C, Grose R, Quondamatteo F, et al. Skin and hair follicle integrity is crucially dependent on beta 1 integrin expression on keratinocytes. EMBO J 2000; 19: 3990–4003. [PubMed: 10921880]
19. Bagutti C, Speight PM, Watt FM. Comparison of integrin, cadherin, and catenin expression in squamous cell carcinomas of the oral cavity. J Pathol 1998; 186: 8–16. [PubMed: 9875134]

20. Downer CS, Watt FM, Speight PM. Loss of alpha 6 and beta 4 integrin subunits coincides with loss of basement membrane components in oral squamous cell carcinomas. J Pathol 1993; 171: 183–190. [PubMed: 8277367]
21. Ferreira M, Fujiwara H, Morita K, et al. An activating beta1 integrin mutation increases the conversion of benign to malignant skin tumors. Cancer Res 2009; 69: 1334–1342. [PubMed: 19190332]
22. Mohr U. International classification of rodent tumors. The mouse. Springer Science & Business Media, 2013.
23. Billings SD, Southall MD, Li T, et al. Amphiregulin overexpression results in rapidly growing keratinocytic tumors: an in vivo xenograft model of keratoacanthoma. Am J Pathol 2003; 163: 2451–2458. [PubMed: 14633617]
24. Li L, Dang Y, Zhang J, et al. REGgamma is critical for skin carcinogenesis by modulating the Wnt/beta-catenin pathway. Nat Commun 2015; 6: 6875. [PubMed: 25908095]
25. Goldenring JR. A central role for vesicle trafficking in epithelial neoplasia: intracellular highways to carcinogenesis. Nat Rev Cancer 2013; 13: 813–820. [PubMed: 24108097]
26. Cheng KW, Lahad JP, Kuo WL, et al. The RAB25 small GTPase determines aggressiveness of ovarian and breast cancers. Nat Med 2004; 10: 1251–1256. [PubMed: 15502842]
27. Yin YX, Shen F, Pei H, et al. Increased expression of Rab25 in breast cancer correlates with lymphatic metastasis. Tumour Biol 2012; 33: 1581–1587. [PubMed: 22644676]
28. Jeong BY, Cho KH, Jeong KJ, et al. Rab25 augments cancer cell invasiveness through a β1 integrin/EGFR/VEGF-A/Snail signaling axis and expression of fascin. Experimental & molecular medicine 2018; 50: e435. [PubMed: 29371698]
29. Amornphimoltham P, Rechache K, Thompson J, et al. Rab25 regulates invasion and metastasis in head and neck cancer. Clin Cancer Res 2013; 19: 1375–1388. [PubMed: 23340300]
30. Clausen MJ, Melchers LJ, Mastik MF, et al. RAB25 expression is epigenetically downregulated in oral and oropharyngeal squamous cell carcinoma with lymph node metastasis. Epigenetics 2016; 11: 653–663. [PubMed: 27379752]
31. Tong M, Chan KW, Bao JY, et al. Rab25 is a tumor suppressor gene with antiangiogenic and anti-invasive activities in esophageal squamous cell carcinoma. Cancer Res 2012; 72: 6024–6035. [PubMed: 22991305]
32. Tellez-Gabriel M, Arroyo-Solera I, Leon X, et al. High RAB25 expression is associated with good clinical outcome in patients with locally advanced head and neck squamous cell carcinoma. Cancer Med 2013; 2: 950–963. [PubMed: 24403269]
33. Pellinen T, Ivaska J. Integrin traffic. J Cell Sci 2006; 119: 3723–3731. [PubMed: 16959902]
34. Watt FM, Jones PH. Expression and function of the keratinocyte integrins. Dev Suppl 1993: 185–192. [PubMed: 8049472]
35. Fuchs E. Skin stem cells: rising to the surface. J Cell Biol 2008; 180: 273–284. [PubMed: 18209104]
36. Rodius S, Indra G, Thibault C, et al. Loss of alpha6 integrins in keratinocytes leads to an increase in TGFbeta and AP1 signaling and in expression of differentiation genes. J Cell Physiol 2007; 212: 439–449. [PubMed: 17474077]
37. Grose R, Hutter C, Bloch W, et al. A crucial role of beta 1 integrins for keratinocyte migration in vitro and during cutaneous wound repair. Development 2002; 129: 2303–2315. [PubMed: 11959837]
38. De Franceschi N, Hamidi H, Alanko J, et al. Integrin traffic - the update. J Cell Sci 2015; 128: 839–852. [PubMed: 25663697]
39. Lathia JD, Gallagher J, Heddleston JM, et al. Integrin alpha 6 regulates glioblastoma stem cells. Cell Stem Cell 2010; 6: 421–432. [PubMed: 20452317]
40. Wang L, Shi ZM, Zhang CQ, et al. Trimalleolar fracture with involvement of the entire posterior plafond. Foot Ankle Int 2011; 32: 774–781. [PubMed: 22049863]

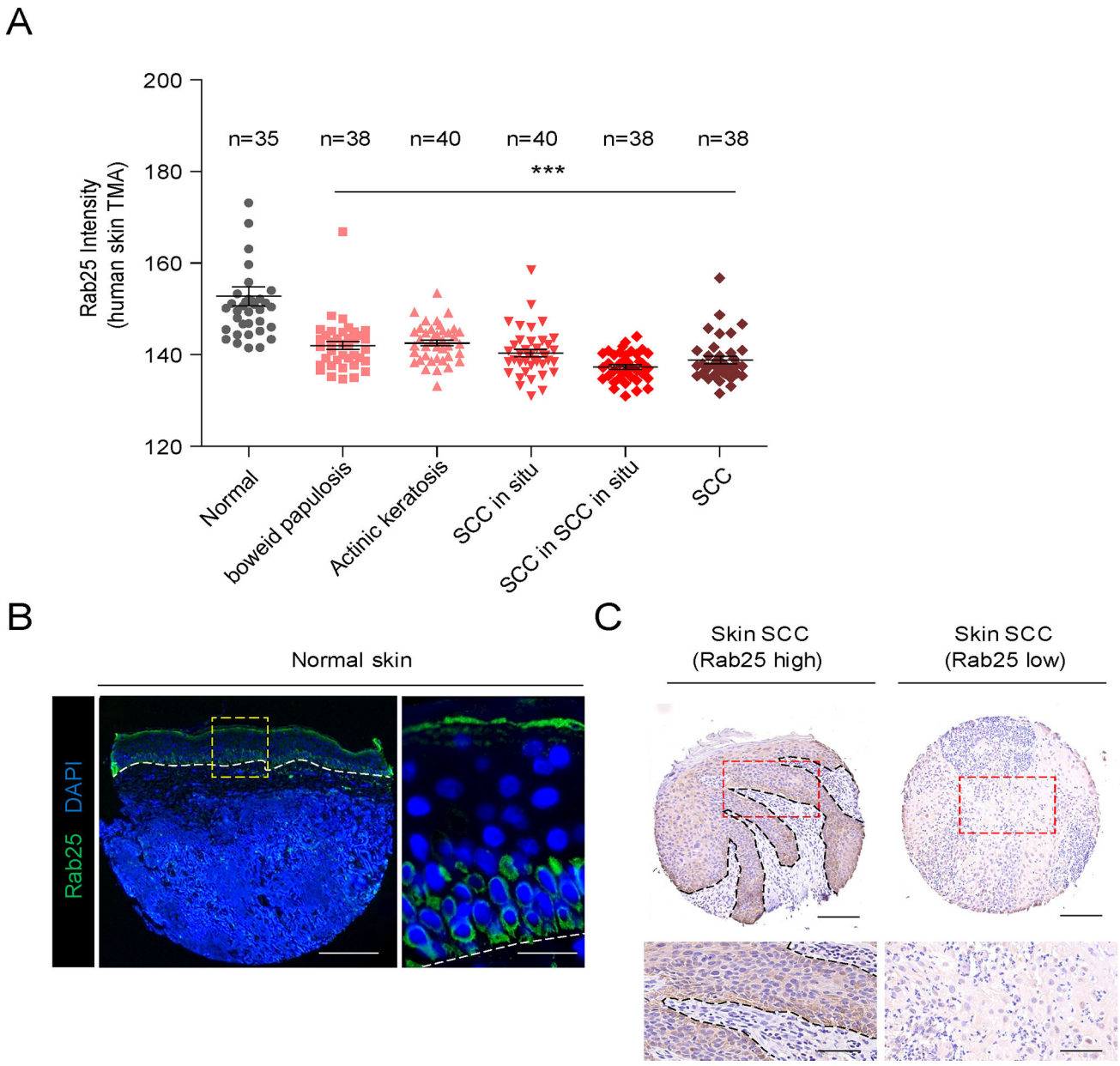

Figure 1.

Rab25 expression of human skin tumor. (A) staining intensity quantitation of Rab25 in a cohort of patients with skin lesions using human skin cancer tissue microarray (TMA). “n” above indicates number of patients. Data represent mean ± SEM. (one-way ANOVA with Dunnett’s multiple comparison, ***$p<0.001$) (B) Representative immunofluorescence image of Rab25 (Green) in human normal skin. Scale bar: 100 μm (left panel); 20μm (right panel). (C) Representative immunohistochemistry image of Rab25 in human skin squamous cell carcinoma (SCC). Scale bar: 100 μm (upper panels); 20 μm (lower panels).

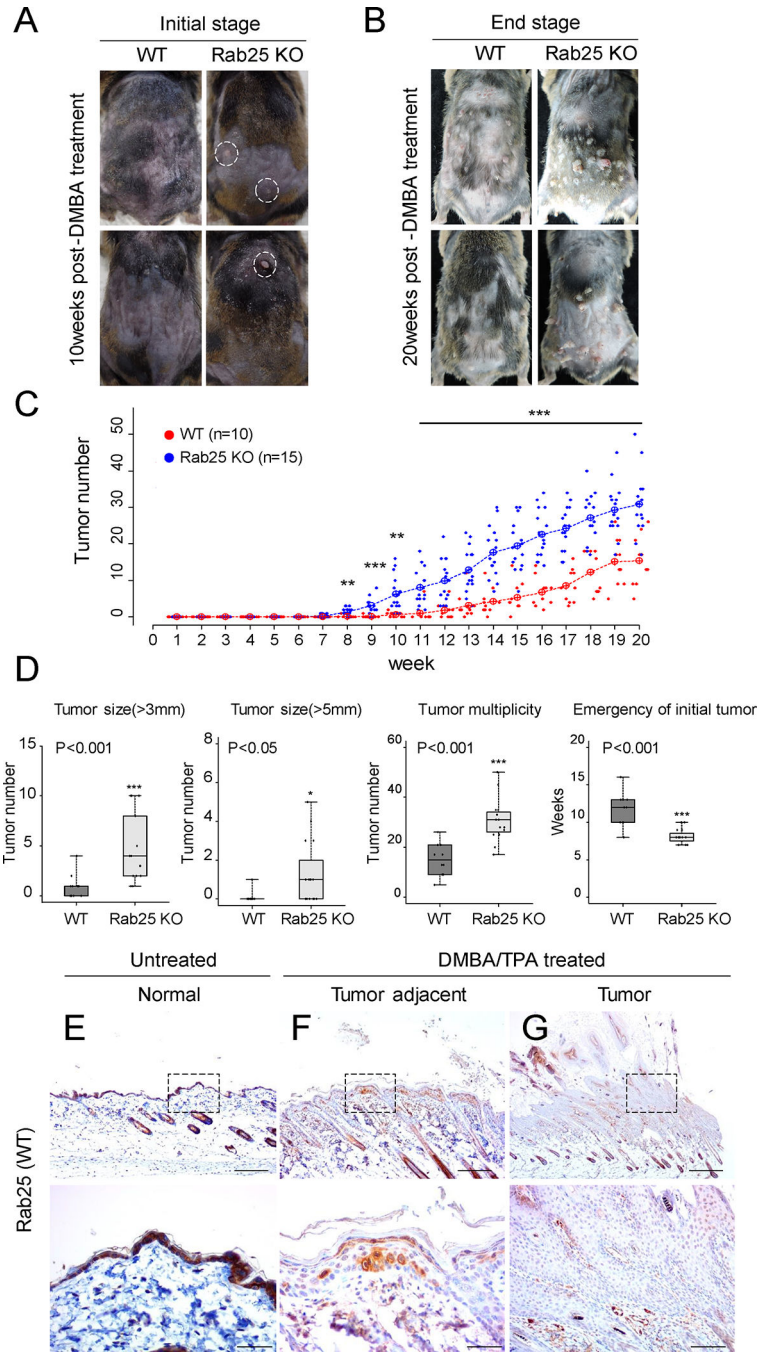

Figure 2.

Susceptibility of Rab25 knock-out mice to the two-stage skin carcinogenesis model. (A) Macroscopic appearance of the dorsal skin of wild type or Rab25 KO mice at 10 weeks post-DMBA treatment. The dotted circles indicate tumors. (B) Macroscopic appearance of the dorsal skin of wild type and Rab25 KO mice at 20 weeks post-DMBA treatment (terminal stage). (C) Skin tumors were counted for WT (red dot) and Rab25 KO mice (blue dot) every week after DMBA treatment until 20 weeks of tumorigenesis as number of tumors per a mouse. (Unpaired student's t test, **p<0.01 ***p<0.001) (D) The average number of tumors

according to diameter (>3 mm: diameter over 3 mm, >5 mm: diameter over 5 mm), total number of tumors (tumor multiplicity) and the average week of appearance of initial tumor (Unpaired student's t test, *p<0.05 ***p<0.001). All tumors in mice were measured by digital calipers every week under anesthesia. (E-G) Rab25 expression in the skin epidermis of untreated and DMBA/TPA treated (end stage) WT mice. Immunostaining intensity of Rab25 in (E) Untreated WT mice with 129J background, (F) epidermis of adjacent tumor (squamous cell hyperplasia). (G) No staining was observed in the whole epidermis of tumor region. Lower panel of E-G show higher magnification views. Scale bar: 200μm (G); 100 μm (E,F); 50 μm (lower panel of F,G); 20 μm (lower panel of E).

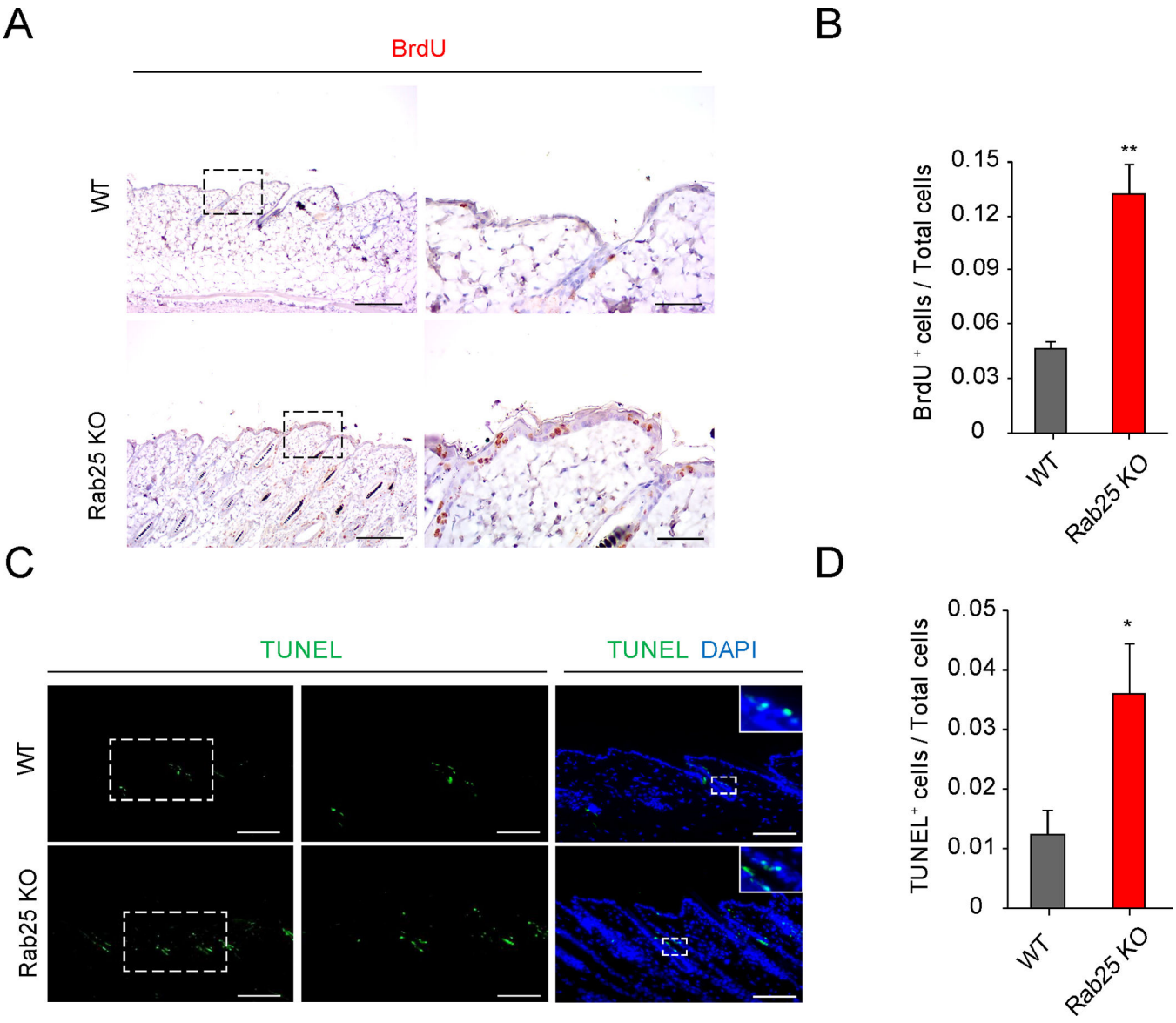

Figure 3.

Characteristics of untreated Rab25 KO mouse skin. (A) Representative image of S-phase BrdU-positive cells in the untreated skin epidermis. Scale bar: 200 μm (left panels); 20 μm (right panels). (B) Quantitation of S-phage proliferating cells. Total cells mean the number of epidermal cells. (Unpaired student's t test, **$p<0.01$) (C) Representative image of TUNEL immunofluorescence staining in the untreated skin epidermis. Scale bar: 200 μm (left panels); 100 μm (other panels). (D) Quantitation of TUNEL positive cells in the epidermis (Unpaired student's t test, *$p<0.05$).

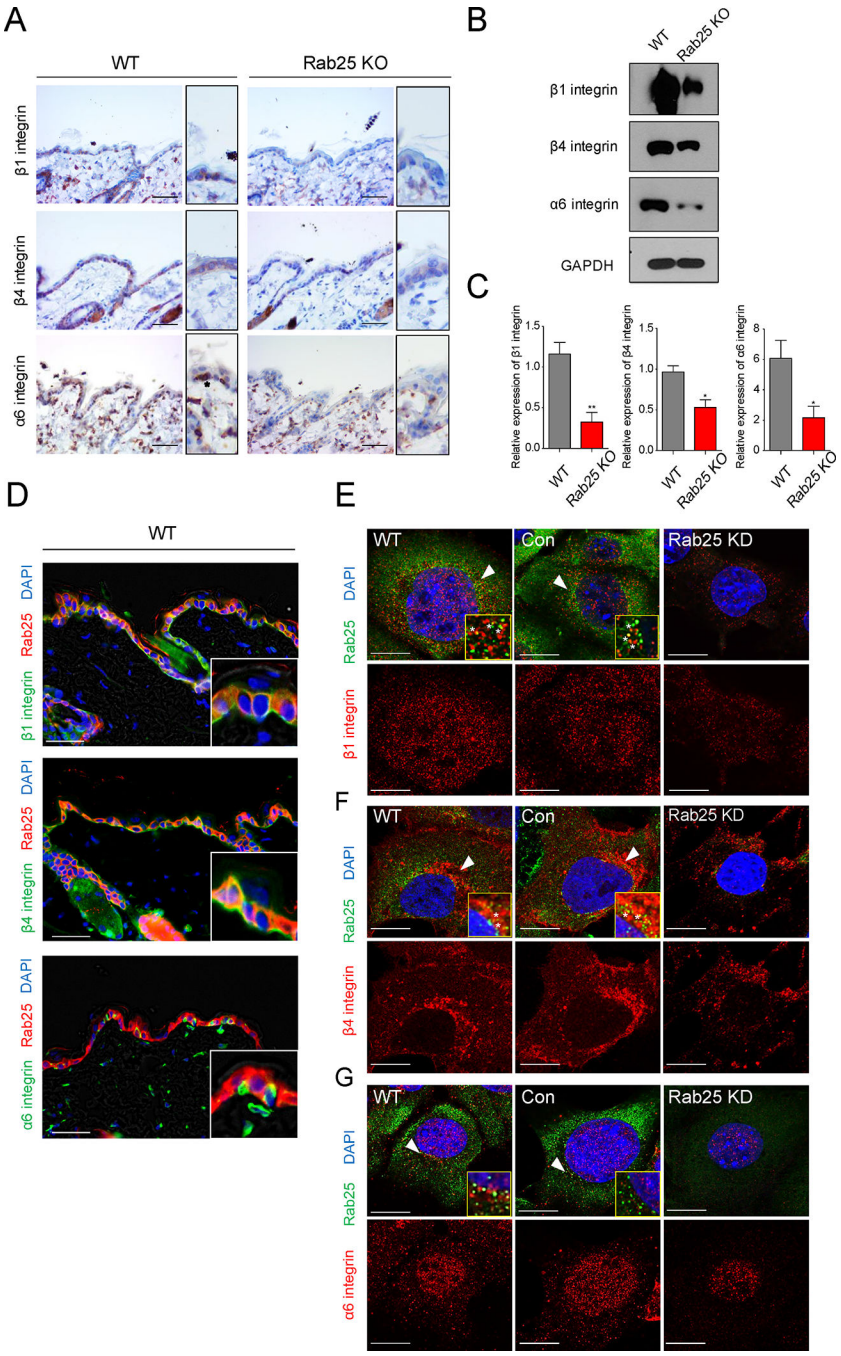

Figure 4.

Alteration of integrin distribution of Rab25 KO mouse and Rab25 deficient keratinocyte. (A) Integrin localization and expression in the intact skin of WT and Rab25 KO mice. Right panel indicates higher magnification of epidermis region. Scale bar: 20 μm. (B) Western blot for integrin β1, β4, and α6 of the skin of WT and Rab25 KO mice. (C) Densitograms of blots. Data represent mean ± SEM. (Unpaired student's t test, n=4 *p<0.05 **p<0.01) (D) Immunofluorescence image of Rab25 (red) and integrin (green) in skin of untreated WT mice. Overlapped panel on merge image (bottom right corner) indicated higher

magnification image of basal cells. Scale bar: 50 μm. (E-G) Localization and expression of Rab25 and integrin was examined by immunocytochemistry staining in WT, control (pGIPZ expressing) and Rab25 knock-down HaCaT cell lines. (E) β1 integrin (red) is co-localized with Rab25 (green) in perinuclear region. (F) β4 integrin (red) is densely localized on perinuclear region and shows co-localization with Rab25 (green) in perinuclear region. (G) α6 integrin (red) was localized on nucleus and sparsely detected in cytoplasm while co-localization with Rab25 (green) was not observed in perinuclear region. Yellow-lined panel indicated higher magnification of perinuclear region. All images were captured by LSM800. Scale bar: 100 μm.

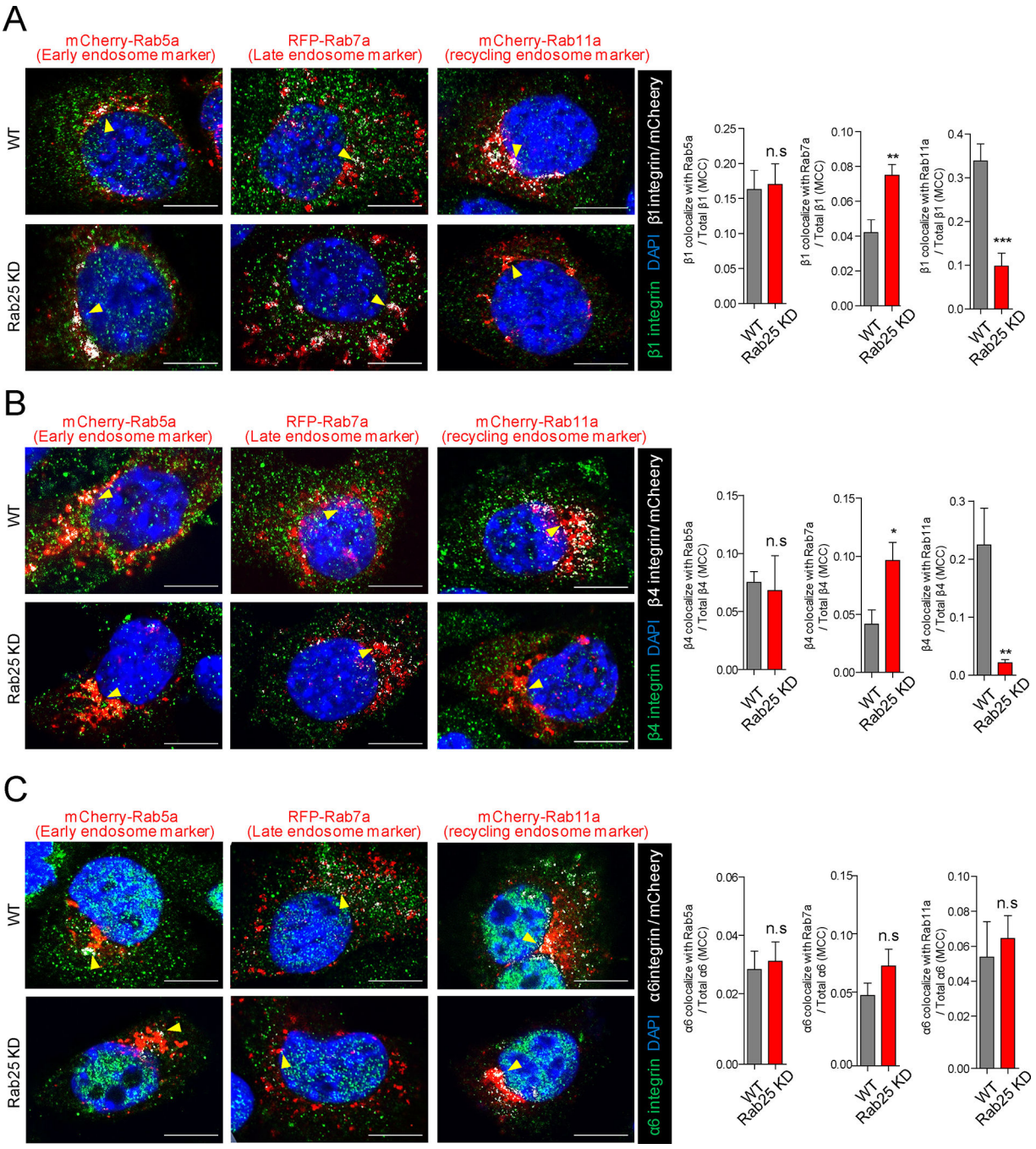

Figure 5.

Alteration of integrin trafficking pathway in Rab25 knock-down keratinocyte. Proportion of integrin (green) co-localized with endosome markers (red): mCherry-Rab5a, RFP-Rab7a, mCherry-Rab11a was examined by immunocytochemistry staining in WT and Rab25 knock-down HaCaT cell lines. All images were captured by LSM780 and analyzed by module of co-localization assay in Zeiss 2012 black edition. (A-C) Representative analyzed confocal image and each yellow arrow indicates co-localization (white pixels). All colocalization was

calculated by MCC (Mander's Colocalization Coefficients, Unpaired student's t test, *p<0.05 **p<0.01 ***p<0.001) Scale bar: 100 μm.

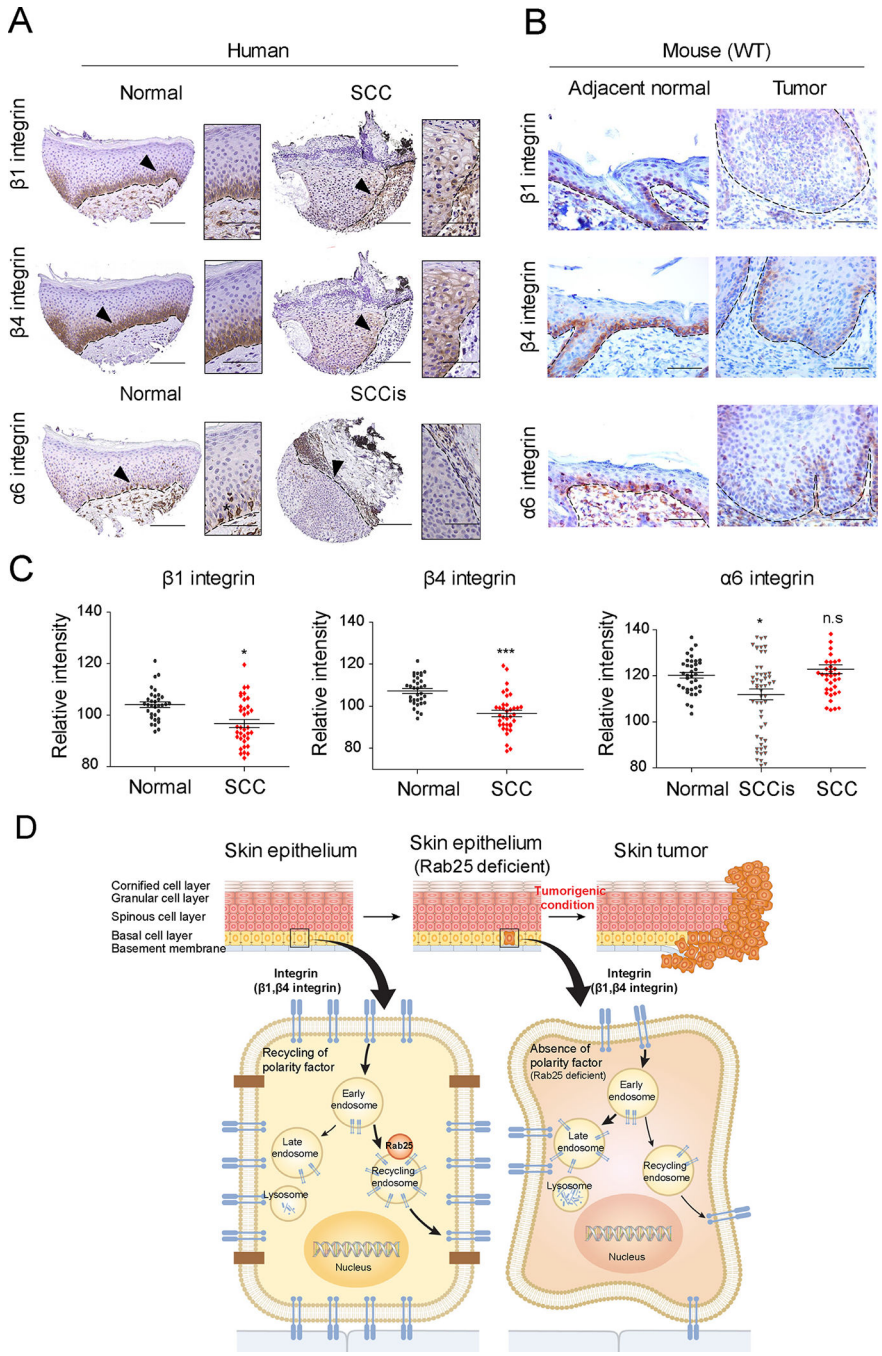

Figure 6.

Reduced expression of β1, β4, α6 integrin in the skin tumor region compared with normal skin region. (A) Representative immunostaining image of integrin (β1, β4, α6) in the human skin squamous cell carcinoma TMA. Black-lined panels indicate higher magnification of basal layer. Scale bar: 50 μm (left panel); 10 μm (right panel). (B) Representative immunostaining image of integrin (β1, β4, α6) in DMBA/TPA treated mice skin. Expression and localization patterns of integrin were identical to those in human skin specimen. Scale bar: 20 μm. (C) Immunostaining intensity of integrin (β1, β4, α6) in a cohort of patients

with skin squamous cell carcinoma lesions. (Unpaired student's t test, *p<0.05 **p<0.01) (D) Graphical image of Rab25 role in keratinocyte. A normal keratinocyte of basal cell (ivory cell) showed abundant population of integrin in cytoplasm and membrane compartment and Endosomal distribution of integrin was highly focused on recycling endosome (blue) compared with late endosome (red). A Rab25 deficient keratinocyte (yellow cell) showed scarcity of integrin population resulting from the increase in integrin distribution into late endosomes along with the marked decrease in integrin distribution in recycling endosomes. Those cells with absence of polarity factors are vulnerable to tumorigenic condition and promote SCC.

Table 1.

Skin lesions Incidence in skin carcinogenesis model.

Mice	Group	No.of skin lesion-bearing mouse		
		Hyperplasia	Papilloma	SCC
WT (n=4)	TPA treated	4	-	-
Rab25 KO (n=4)		4	2	-
WT (n=10)	DMBA/TPA treated	10/10	10/10	1/10
Rab25 KO (n=15)		15/15	15/15	9/15 **

unpaired Student's t test,

** p<0.01

Author Manuscript

Author Manuscript

Author Manuscript

Table 2.

Increment of malignancy in Rab25 KO mouse.

Mice	Group	No.of lesions / mouse		
		Hyperplasia	Papilloma	SCC
WT (n=4)	TPA treated	1.8±0.5	-	-
Rab25 KO (n=4)		4.5±0.3	0.8±0.5	-
WT (n=10)	DMBA/TPA treated	8.0±0.7	7.4±1.0	0.1±0.1
Rab25 KO (n=15)		9.5±0.8	16.1±1.3***	1.27±0.3**

unpaired Student's t test,

** p<0.01

*** p<0.001